in *Rock Mechanics in the National Interest*, ed. by D. Elsworth, J.P. Tinucci, and K.A. Heasley, 205-210, Balkema, 2001

Simulation of immiscible viscous displacement within the plane of a horizontal fracture

M.J. Nicholl
University of Idaho, Moscow, Idaho, USA

R.J. Glass
Sandia National Laboratories, Albuquerque, New Mexico, USA

ABSTRACT: We consider the use of a modified diffusion-limited aggregation (DLA) process to model immiscible viscous displacements in rough-walled fractures. We include the effects of local aperture field variability to channelize flow within a fluid phase and capillarity to smooth the displacement front. Model behavior is illustrated over a limited set of simulations in both a Hele-Shaw cell, and a variable aperture field that is correlated well below the simulation scale.

1 INTRODUCTION

The issue of immisicble displacement of one fluid by another rises in the context of enhanced oil recovery, remediation of nonaqueous phase liquids, CO_2 sequestration, and other applied geologic problems. In discrete fractures, accessibility will combine with competition between capillary, gravity, and viscous forces to control the displacement process. Here we focus on behavior in a single horizontal fracture at the sub-meter scale for conditions where viscous forces cannot be ignored. Immiscible displacement processes can (and have been) modeled using a number of different approaches that may be broadly categorized as continuum or discrete. In continuum approaches, one either: 1) solves the Navier-Stokes equations for each fluid within complex geometry, and separated by a moving boundary where kinetic and dynamic boundary conditions must be met; or, 2) describes the system as a two-phase continuum with relative permeability and pressure-saturation relations defined for both fluids at every point. In the discrete approaches, a set of local 'rules' are applied to model pore-scale behavior; broad categories of rules include: 1) Particle interaction models (PIM) such as cellular automata, lattice-Boltzman, or lattice-gas where large quantities of particles simultaneously move and interact according to a list of rules; 2) Invasion percolation (IP) where individual apertures along the fluid-fluid interface are filled according to local accessibility and capillary criteria; and, 3) Diffusion-limited aggregation (DLA) in which random particles moving through the displaced fluid are used to identify locations on the interface for advancement.

Both the Navier-Stokes and PIM approaches are currently limited by the difficulty of defining the fluid-fluid interface, and computational requirements at our scale of interest. Two-phase continuum approaches are computationally tractable, but do not correctly include the physics of displacement processes; i.e. the fluid phases intermingle where they should be separate. IP and DLA have potential at the scale of interest, both are growth models that encapsulate the critical unit process (aperture filling), and iterate that process to yield large scale behavior. The basic IP process models capillary dominated horizontal displacements on a random aperture field. However, IP has recently been modified to include gravity and the dynamic calculation of interfacial curvature at the fluid-fluid interface within a fracture (e.g. Glass, 1993, Glass et al., 1998). The latter, termed MIP, yields simulated behavior that matches experimental measurements quite well. In addition, there have also been recent attempts to further include viscous forces in IP or MIP (Xu et al., 1998, Ewing & Berkowitz, 1998) with excellent correspondence to experiments in heterogeneous porous media where capillary, gravity, and viscous forces all played a role (Glass et al., in press).

Here we focus on a DLA based approach for simulating fluid-fluid displacement. The DLA process begins with a cluster that consists of a single occupied grid block at the center of a large regular lat-

tice (Witten & Sander, 1981). A particle introduced at a random location far from the cluster walks randomly on the lattice until it contacts either the cluster or a system boundary. On contacting a boundary, the particle dies and is replaced by another; however, if it enters a grid block adjacent to the cluster, the particle stops, and that grid block joins the cluster; the process is then repeated until some criteria is met (e.g. cluster size, number of particles). It was later shown that this simple model acts as a solution to the LaPlace equation (Witten & Sander, 1983), and is consistent with miscible displacement of a viscous fluid by an inviscid one in the limit of no mixing (Paterson, 1984).

Our objective is to develop a DLA based model for immiscible displacement within a rough-walled fracture that incorporates: (1) full spectrum of viscous behavior from viscous stabilized to viscous destabilized (especially in transition); (2) influence of capillary forces at the fluid-fluid interface; and (3) the critical influence of aperture variation to create complexity due to both capillarity at the phase interface and channeling of flow within each phase. Sideiqui & Sahimi (1990) partially addressed (1), and others (e.g. Vicsek, 1984, Szep et al., 1985, Kadanoff, 1985) have explored (2); however, neither issue has been solved, and the literature appears to be silent on (3). In this paper, we begin model development by focusing on the influence of capillary forces at the fluid-fluid interface, and in the context of only local roughness induced influence on flow.

2 MODEL DEVELOPMENT

The model suggested here is like DLA in that the cluster of grid blocks representing the displacement front grows in discrete steps at locations identified by independent particles moving through the displaced fluid; particles are not allowed to enter, nor move through the displacing fluid. A first principle difference from DLA, is that particles move through the displaced fluid on off-lattice random trajectories biased according to local transmissivity. In this way, we allow local aperture geometry to influence growth of the displacement front by focusing particles into conductive zones. A second principle difference from DLA is in how we identify "sticking" between a moving particle and the growing cluster. Cluster growth in the original DLA model is promiscuous, in that all particles contacting the cluster "stick" and became part of it; this leads to highly ramified and fractal clusters dominated by noise. In order to increase resemblance to fluid-fluid displacement (i.e. produce more compact structures), a number of authors have suggested modifying the conditions under which a particle sticks to the cluster.

Of particular interest are sticking rules that approximate the effects of surface tension by considering local cluster density as an analog to interfacial curvature in the fracture plane (e.g. Vicsek, 1984, Kadanoff, 1985, Szep et al., 1985). We incorporate the effects of interfacial curvature at first order by only allowing particles contacting the cluster to stick if local density exceeds a predetermined criteria (k). In our model, "nearest neighbors" to the site being considered are given more weight than portions of the cluster further away. Figure 1 shows a site (black dot) being considered as a candidate for membership in the adjacent cluster (gray blocks). First, we center a box of size b x b on the candidate site (b = 5 in Figure 1, and must be an odd number). Within that box, we then calculate a weighting factor (w) for each site occupied by the cluster; weights are given by the inverse radial distance between that site and the candidate site ($w = 1/r$), which for Figure 1, would be 1/1, $1/\sqrt{2}$, and $1/\sqrt{3}$. We then sum the values of w, and normalize the total to the sum of all possible values of w within the box. If this normalized measure of interfacial curvature exceeds our predetermined criteria (k), the particle sticks, otherwise the particle dies and a new one is started. Standard DLA corresponds to k = 0, and the influence of interfacial tension increases with k. The upper limit on k (k_{max}) is dependent on geometry of the cluster seed; in order for growth to begin, k_{max} must be small enough to allow sticking at the seed. We also note that this model does not include restructuring of the cluster in the vicinity of contact, as has been suggested by others (e.g. Vicsek, 1984, Kadanoff, 1985). Finally, size and shape of the box are adjusted to accommodate sites near the side boundaries.

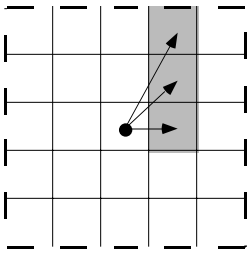

Figure 1: Interfacial curvature is estimated at first order by calculating density of the cluster (gray blocks) within a box (dashed lines) centered on the grid block being considered for membership in the cluster (marked with a dot). Relative influence of various sites in estimating interfacial curvature is inversely proportional to distance from the site under consideration (see arrows).

3 MODEL IMPLEMENTATION

Displacement from a fracture edge is simulated by configuring our simulation domain as shown in Figure 2. A seed for the growing cluster is established by filling a strip of blocks along one edge with the displacing fluid (e.g. Kadanoff, 1985, Flury & Fluhler, 1995); all remaining blocks are initially occupied by the fluid being displaced. Particles are started from randomly selected locations along a "release line" that is parallel to the seed (Fig. 2), and separated from the growing cluster by a distance (d). As the cluster grows, the release line is moved in the x direction to maintain that separation. For computational expediency, particles that wander to a distance of 2d from the cluster tip in the x direction are destroyed, and a new particle started; this destructive boundary is also moved with cluster growth. Long edges of the system (Fig. 2) are designated as refusal boundaries; movement across these boundaries is disallowed, the particle must make another (random) choice. The refusal boundary condition could also be described as elastic reflection without conservation of momentum. Finally, because particles are not allowed to enter the displacing fluid, particle interactions with the left-hand boundary are irrelevant.

Particle movements are made off-lattice in steps one grid block in length. For every step, the unit displacement vector is determined by resolving component vectors in the four directions (+x, -x, +y, -y). Each component vector is calculated by choosing a random number (0 to 1) and multiplying it by the local transmissivity in that direction. The particle is then moved according to the displacement vector, unless doing so would initiate contact with a boundary or the cluster. This process is repeated until the particle contacts the cluster, a boundary, or dies. In a variable transmissivity field, a particle could become effectively trapped between a material heterogeneity and a refusal boundary. In order to preclude infinite loops, particles are allowed a limited number of moves (including attempts) before they are destroyed and replaced by a new particle.

4 ILLUSTRATIVE SIMULATIONS

The model described above was exercised over a range of values for k on two transmissivity fields: a parallel plate geometry (Hele-Shaw cell) and a variable-aperture field originally measured by Nicholl et al. (1999). The variable-aperture field had stationary spatial statistics similar to those given by an exponential function, with a coefficient of variation equal to 0.24, and well defined spatial correlation length. For computational expediency, we limited our simulations to a 300 x 400 subset (~56 x 75 correlation lengths) of the measured field (see Fig. 3); the Hele-Shaw cell was also explored over a 300 x 400 grid.

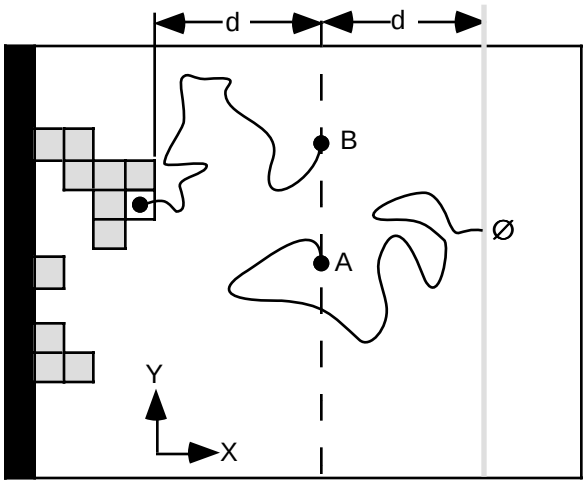

Figure 2: Model conceptualization on a rectangular grid. Black grid blocks along the left side represent the seed, gray blocks are the growing cluster, and solid lines (right side, top and bottom) represent system boundaries. Particle A is started from the release line (dashed line) located a distance d from the tip of the growing cluster, and then walks about the domain (see rules in text). Upon reaching a distance of 2d from the cluster tip (gray line), particle A is destroyed, and a new one released. Particle B reaches an empty grid block adjacent to the cluster. This grid block will be considered for membership in the cluster if the next step of particle B would take it onto the cluster.

In a small difference from DLA (e.g. Kadanoff, 1985), we defined contact as an attempt by the moving particle to walk onto the cluster from an adjoining grid block (contact point). Box size (b) for calculating cluster density was arbitrarily set to look ten grid blocks in each direction from the contact point (b = 21). To correspond with our choice for b, the seed filled the first 10 columns of each array, (b - 1)/2 = 10; this configuration sets k_{max} = ~0.46. Distance between the cluster tip and release line (d) was set at 25 grid blocks, which is about 4.5 times the correlation length of the variable-aperture fields. This value was chosen as a trade-off between introduction of artifacts and computational efficiency. Much smaller values for d altered model outcome significantly, while much larger values led to an exponential increase in computation time. In each fracture, a single realization was performed at k = 0, and increasing values of k in increments of 0.05. In the Hele-Shaw cell, simulations were run for k = 0 to 0.46; due to time constraints, we were unable to complete simulations for k > 0.35 in the variable-aperture fracture.

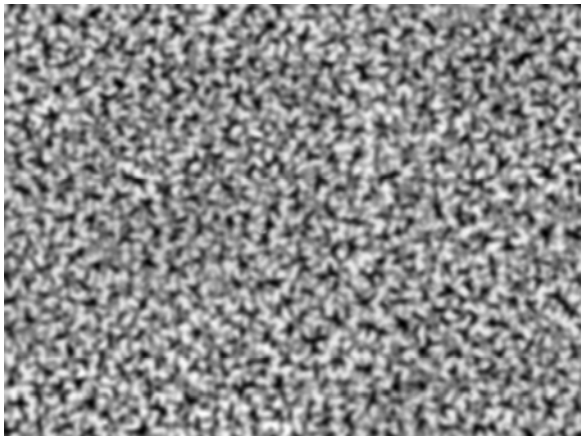

Figure 3: Variable-aperture field considered here is a 300 x 400 grid block subset of an aperture field measured by Nicholl et al. (1999) using techniques presented by Detwiler et al. (1999). Light shades represent large apertures and dark shades small ones.

5 RESULTS

Simulations demonstrate that both transmissivity induced bias and k based capillarity have first-order influences on phase invasion structure (Fig. 4). For k = 0, the growth process leads to a highly ramified structure with densely packed branches. Conversely, the structure formed at k = 0 in the variable-aperture field is much more open, with little small-scale branching; intermediate-scale branches make numerous sharp changes in direction and are separated by distances on the order of the aperture correlation scale or larger. The end result is a structure that could best be described as a backbone. As k increases, branch tips in the Hele-Shaw cell begin to close, and encircle portions of the displaced fluid; in the variable-aperture field, branches become thicker and denser, but generally remain separate. At larger values of k (k = 0.20), interfacial curvature dominates cluster growth in the Hele-Shaw cell; branched structures coalesce to form smooth rounded fingers, tip splitting reduces, and fingers become increasingly straight. In the variable-aperture fracture, a similar process is seen, however with a local correlation superimposed. Branches become increasingly smooth and thicker at the local scale and then begin to coalesce to form large scale fingers of roughly the same scale as seen in the Hele-Shaw cell (compare simulations at k = 0.35). Note that the entrapped phase saturation is nearly identical, but the structure is quite different between the two at k = 0.35 (see below). At the largest value of k considered (0.46), fingers within the Hele-Shaw cell merged to form a flat front; insufficient time was available to run similar simulations in the variable-aperture field.

In both fractures, the growing cluster surrounds and entraps portions of the displaced fluid. We define the areal saturation as the number of sites occupied by the cluster relative to the total number within the bounds of the cluster (occupied plus entrapped displaced fluid). Areal saturation is lower in the Hele-Shaw cell than the variable-aperture field at all values of k considered (Fig. 5). There is also a significant change in behavior at intermediate values of k, as areal saturation first decreases sharply then increases. Between k = 0.10 and k = 0.15, intermediate scale branches in the Hele-Shaw cell begin to join at the tips, entrapping relatively large areas within the growing cluster. At higher values of k, the structure is denser, and branches do not have the opportunity to encircle large areas; hence, trapped areas are smaller (on the order of one to several grid blocks) and areal saturation increases. In the rough-walled fields, branches don't connect on a large scale at low k, so entrapment occurs locally, and to a lesser degree than in the Hele-Shaw cell. However, as k increases, trapping does begin to occur above the correlation length.

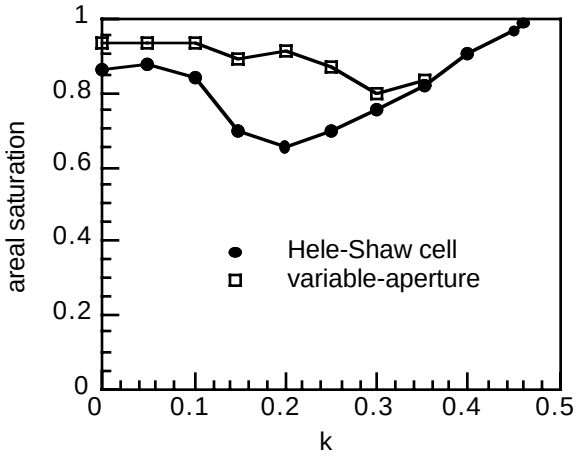

Figure 5: Areal saturation describes the fraction of sites within the cluster bounds that are occupied by the displacing fluid.

As a measure of the computational penalty for considering our k based sticking rule, we define survival rate as the fraction of particles contacting the growing cluster that met the sticking criteria (Fig. 6). At k = 0, the sticking rules are promiscuous, and all particles that make contact stick to the cluster (100% survival). The influence of interfacial curvature shows itself at k > 0.05, where the fraction of particles sticking decreases sharply for the variable-aperture fracture, and less drastically for the Hele-Shaw cell. In the variable-aperture field, heterogeneity will tend to focus particles, rather than let them freely access suitable sites, as occurs in the Hele-

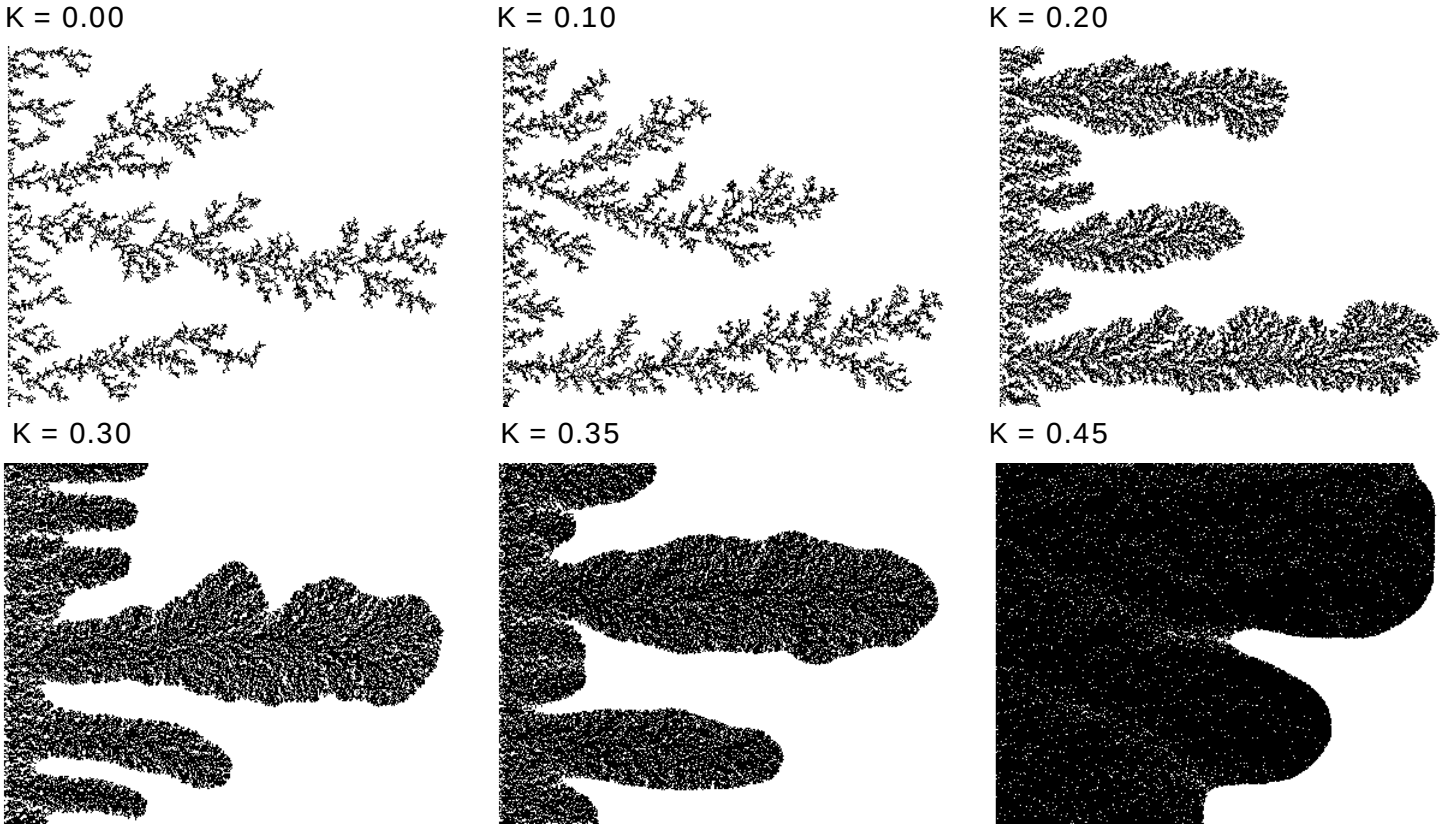

Figure 4: Displacement simulations for the Hele-Shaw cell (above) and variable-aperture fracture (below).

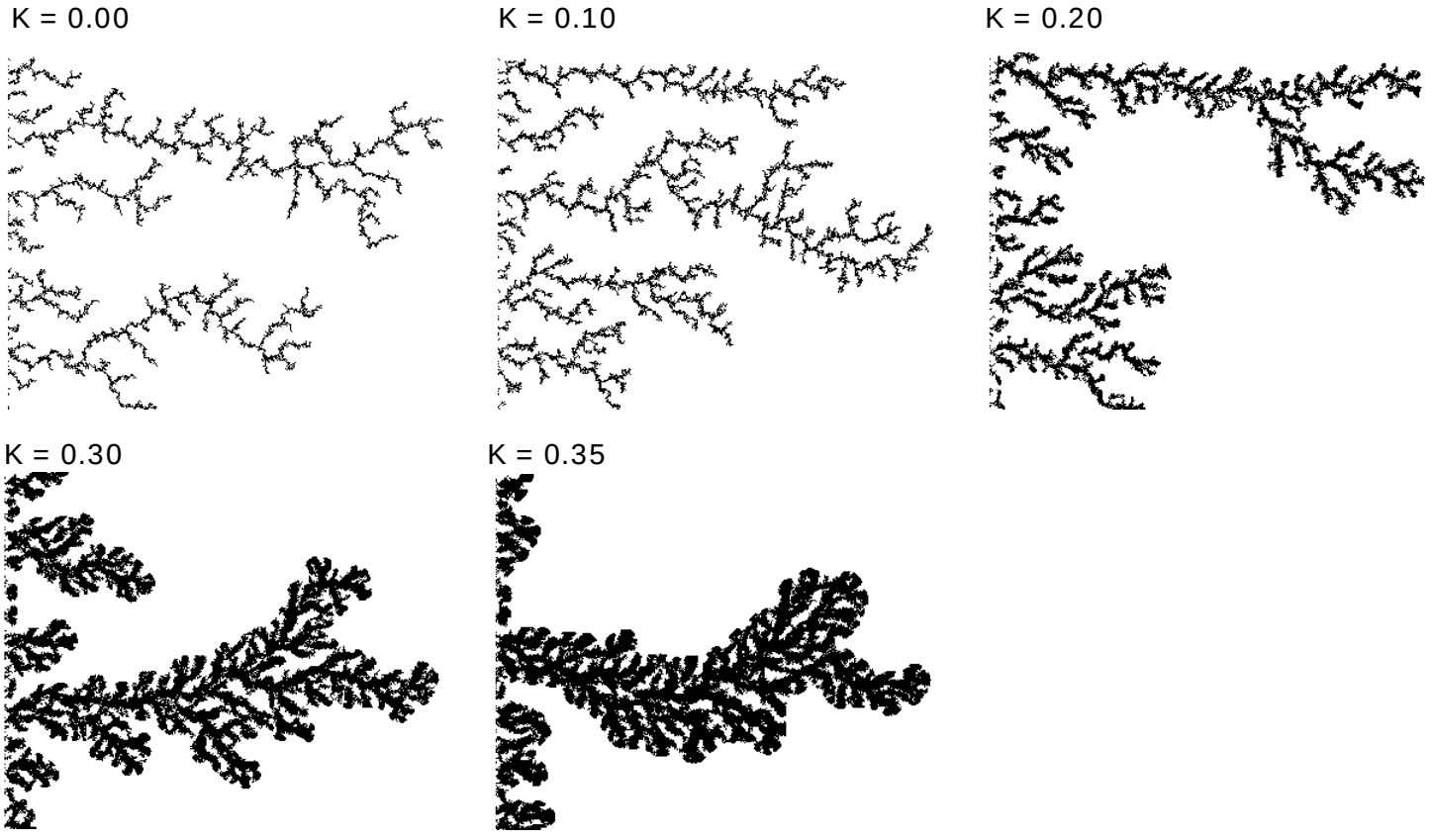

Shaw cell. The inverse relationship between survival rate and computation time precluded presentation of simulations in the variable-aperture field for $k > 0.35$; that work will be completed shortly.

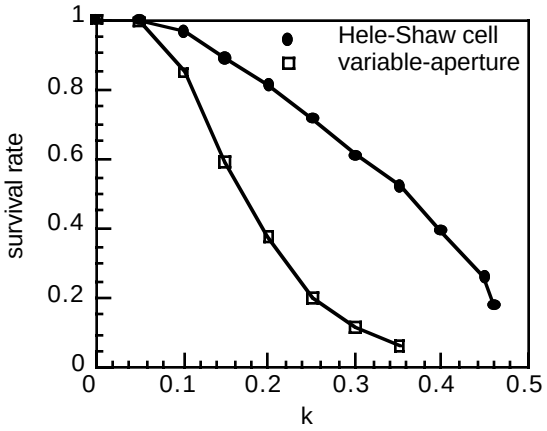

Figure 6: Survival rate describes the fraction of particles contacting the cluster that stick.

6 CONCLUSIONS

Model shows a range of behavior consistent with expectations, and provides an encouraging beginning to modified DLA approaches for simulation of immiscible displacements in variable aperture fractures where viscous forces are important. Local transmissivity bias channels growth into connected large apertures to honor aperture field heterogeneity. A density based sticking rule models capillarity and systematically smoothes the interface. In the Hele-Shaw cell, increasing capillarity at the front leads to increased finger width, as both theory and experiments have found (Homsy, 1987). In combination with local transmissivity bias (variable-aperture field), increasing capillarity first widens fingers within channels, and then causes coalescence to create macroscopic finger structures at scales comparable to those in the Hele-Shaw cell.

ACKNOWLEDGMENTS

Financial support for this work was provided by the U.S. Department of Energy's Basic Energy Sciences Geoscience Research Program under contract numbers DE-FG03-01ER15122 (University of Idaho) and DE-AC04-94AL85000 (Sandia National Laboratories).

REFERENCES

Detwiler, R.L., Pringle, S.E. & Glass, R.J. 1999. Measurement of fracture aperture fields using transmitted light: An evaluation of measurement errors and their influence on simulations of flow and transport through a single fracture. *Water Resources Research*. 35(9): 2605–2617.

Ewing, R.P. & Berkowitz, B. 1998. A generalized growth model for simulating initial migration of dense non-aqueous phase liquids. *Water Resources Research*. 34(4): 611-622.

Flury, M. & Fluhler, H. 1995. Modeling solute leaching in soils by diffusion-limited aggregation: Basic concepts and application to conservative solutes. *Water Resources Research*. 31(10): 2443-2452.

Glass, R.J. 1993. Modeling gravity-driven fingering in rough-walled fractures using modified percolation theory. *Proceedings of the Fourth Annual International Conference on High Level Radioactive Waste Management*, Las Vegas, April 26-30 1993. 2042-2052. LaGrange Park, Illinois: American Nuclear Society.

Glass, R.J., Nicholl, M.J. & Yarrington, L. 1998. A modified invasion percolation model for low-capillary number immiscible displacements in horizontal rough-walled fractures: Influence of local in-plane curvature. *Water Resources Research*. 34(12): 3215-3234.

Glass, R.J., Conrad, S.H. & Yarrington, L. in press 2001. Gravity destabilized non-wetting phase invasion in macro-heterogeneous porous media: Near pore scale macro modified invasion percolation model. *Water Resources Research*.

Homsy, G.M. 1987. Viscous fingering in porous media. *Ann. Rev. Fluid Mechanics*. 19: 271-311.

Kadanoff, L.P. 1985. Simulating hydrodynamics: a pedestrian model. *J. Statistical Physics*. 39(3/4): 267-283.

Nicholl, M.J., Rajaram, H., Glass, R.J. & Detwiler, R. 1999. Saturated flow in a single fracture: Evaluation of the Reynolds Equation in measured aperture fields. *Water Resources Research*. 35(11): 3361-73.

Paterson, L. 1984. Diffusion-limited aggregation and two-fluid displacements in porous media. *Physical Review Letters*. 52(18): 1621-1624.

Sideiqui, H. & Sahimi, M. 1990. A statistical model for simulating miscible viscous fingers in porous media and other growth phenomena. *J. Phys. A: Math*. 23: L497-L503.

Szep, J., Cserti, J. & Kertesz, J. 1985. Monte Carlo approach to dendritic growth. *J. Phys. A: Math*. 18: L413-L418.

Vicsek, T. 1984. Pattern formation in diffusion-limited aggregation. *Physical Review Letters*. 53(24): 2281-2284.

Witten, T.A. & Sander, L.M. 1981. Diffusion-limited aggregation, a kinetic critical phenomenon. *Physical Review Letters*. 47: 1400-1403.

Witten, T.A. & Sander, L.M. 1983. Diffusion-limited aggregation. *Physical Review B*. 27(9): 5686-5697.

Xu, B., Yortsos, Y.C. & Salin, D. 1998. Invasion percolation with viscous forces. *Physical Review E*. 57(1): 739-751.